ISSN: 0871-7869

Characterization of 'Gaioleiro' Buildings

A. Simões; R. Bento

- Maio de 2012 -

Relatório ICIST
DTC nº 07/2012

CONTENTS

FIGURE CONTENTS

TABLE CONTENTS

SYMBOLS

γ – Specific Weight

E – Young’s Modulus

G – Shear Modulus

ν – Poisson ratio

ξ – Viscous damping ratio

f_c – Compressive strength

f_t – Tensile strength

τ – Shear strength

τ_o – Cohesion

μ – Coefficient of friction

G’ – Fracture Energy

β – Shear retention factor

1. INTRODUCTION

Old masonry buildings are mainly composed by thick masonry walls arranged in perpendicular planes and relatively flexible wooden floor diaphragms. This report presents a brief description of the masonry 'Gaioleiro' buildings, characteristic of the urban expansion of Lisbon at the end of the nineteenth century and the beginning of the twentieth century.

Built after the 'Pombalino' reconstruction, the 'Gaioleiro' buildings represent a regress on the methods of construction and structural reliability when compared with the preceding masonry buildings. It is believed that this typology of buildings presents the highest seismic vulnerability of Lisbon's old masonry buildings supporting the need of assessing their structural behaviour and the study of retrofitting schemes.

The goal of this work is to gather the available information regarding the period of construction, the materials of construction, the structural system and the general state of conservation, aiming at the qualitative evaluation of the buildings expected behaviour when subjected to the action of earthquakes. This report also includes a review of the studies up-to-date developed about the assessment of 'Gaioleiro' buildings.

2. HISTORIC SURVEY

On November 1st, 1755 Lisbon was hit by a very strong earthquake followed by a tsunami that caused great destruction in the city. The new downtown design placed the buildings in rectangular quarters with similar dimension following an orthogonal grid of streets. During the first half of the nineteenth century there were few changes on the urban landscape as the city continued to grow according with the 'Pombalino' reconstruction plan. In 1864, a commission was nominated by the Ministry of Public Works to deal with a program of urban improvements and expansion of the city to the north upland (Figure 1).

The opening of Liberdade Avenue in 1886 (Figure 2 a) and Almirante Reis Avenue (Figure 2 b), in addition to developments on the east side with 24 de Julho Avenue, improved the connection of the city centre with the rural periphery. In 1888, the engineer Ressano Garcia developed a new plan regarding the connection between Liberdade Avenue and Campo Grande through the opening of Fontes Pereira de Melo Avenue and República Avenue (Figure 2 c).

The 'Gaioleiro' buildings are related with the construction of Bairro de Camões occupying the hill on the east side of Santa Marta Street (Figure 3) and 'Avenidas Novas' adjacent to Fontes Pereira de Melo Avenue and República Avenue (Figure 4). The buildings were aggregated in quarters with interior yards and surrounded by a grid of secondary streets, wider than the streets of the 'Pombalino' downtown. Generally, the quarters have a rectangular shape, though there are also trapezoidal shape quarters conditioned by the slope of the uptown land, originating corner buildings with irregular dimensions.

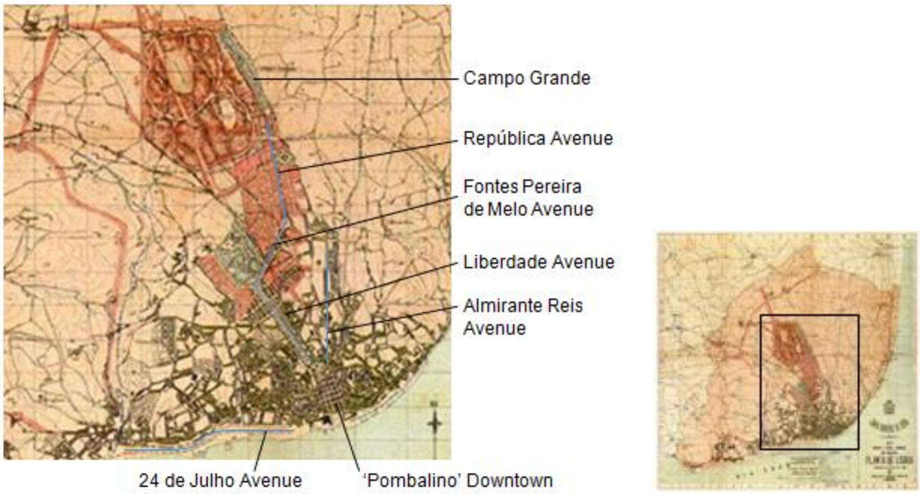

Figure 1 - Plan of Lisbon in 1903 (adapted from AFML).

a) b) c)

Figure 2 – Contemporary pictures (AFML): a) Liberdade Avenue in 1900; b) Almirante Reis Avenue in 1908; c) República Avenue.

Figure 3 – Compounds of 'Gaioleiro' buildings on the east side of Santa Marta Street.

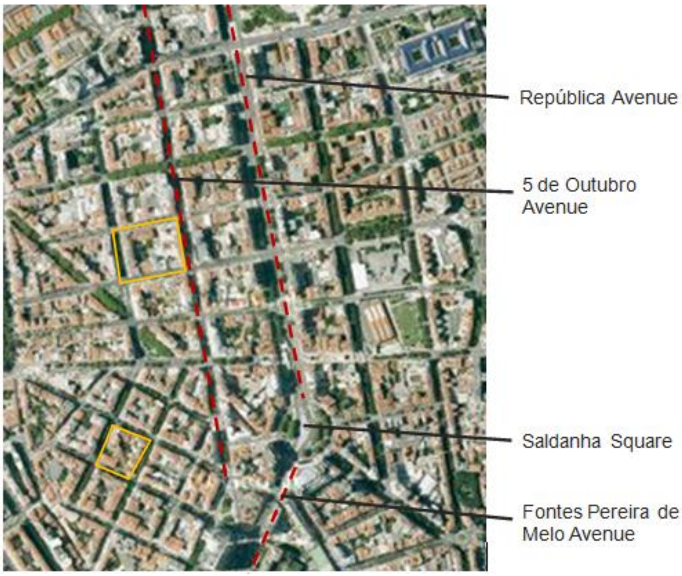

Figure 4 – Compounds of ‘Gaioleiro’ buildings on the east side of Santa Marta Street.

3. DESCRIPTION OF THE BUILDINGS

The new areas of expansion included modest buildings intended to the middle class population and singular buildings displaying the social status of their owners (Figure 5). The ‘Gaioleiro’ buildings are related with the buildings built to be sold or to be rented by flats aiming to sustain the development of the city and the housing needs of an increasing population.

a) b) c)

Figure 5 – Expansion to the north upland (AFML): a) Rentable building from 1895 in Liberdade Avenue; b) Rentable building in Fontes Pereira de Melo Avenue; c) Palatial building from 1906 in Liberdade Avenue.

The expansion program proposed by Ressano Garcia was very flexible compared with the ‘Pombalino’ plan. The construction was carried out by private entities, and therefore the quality of the buildings is very variable as well as the design of the buildings. The buildings are usually longer into the backyard and tighter into the façade walls, originally with two flats per storey or only one, resulting from the division of a larger fraction. The side walls are interrupted by light-shafts to provide natural light and ventilation to the interior rooms (Figure 6).

Figure 6 - Example of light-shafts (Appleton, 2005 and Andrade, 2011).

According to Appleton (2005), the ‘Gaioleiro’ buildings might be divided into four different types: Type 1 – Small to medium size buildings with strait to medium front façade wall, lateral light-shaft, lateral stairs and one flat per floor (Figure 7 a); Type 2 – Large size buildings, with large front façade wall, lateral light-shaft and one flat per floor; Type 3 - Large size buildings, with large front façade wall, two lateral light-shafts and eventually one central light-shaft, central stairs and two flats per floor (Figure 7 b); Type 4 - Large size buildings on the corner of the compound, with two or more light-shafts, central stairs and two or more flats per floor (Figure 7 d). Within the quarter, there are buildings with five storeys (including attic), like the original ‘Pombalino’ buildings, right next to buildings with seven storeys, with generous ceiling height.

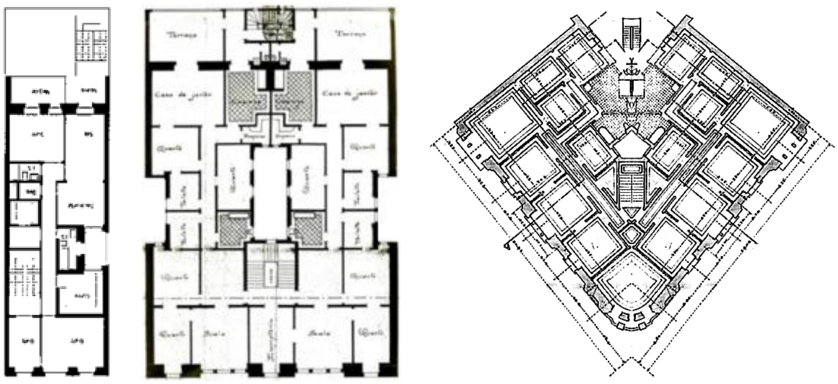

a) b) c)

Figure 7 – Plan of ‘Gaioleiro’ buildings: a) Example of Type 1 (Andrade, 2011); b) Example of Type 3 (Branco, 2007); c) Example of Type 4 (Andrade, 2011).

Figure 8 – ‘Gaioleiro’ buildings with different size and shape.

Contrasting with the ‘Pombalino’ reconstruction plan, there were no standards for buildings height or depth, neither for the architectural design of the façade walls. The front façades were often decorated with a collection of *Art Nouveau* details, windows with laboured stone frames and with different shapes or positions within the floors (Figure 9). Three distinct levels can be identified on the front façade walls: the base masonry cover (often made of plaster instead of masonry), the middle part extensively adorned or covered by ceramic tiles, and the roof with dormer windows (Figure 10).

The back façade walls are recognized by the metallic balconies or galleries and service staircases to access the interior area of the block, which were actually imposed by the fire-fighters and influenced by the contemporary Iron Architecture (Figure 11).

Figure 9 - Decorative details from the front façade wall.

Figure 10 – Dormer windows.

Figure 11 – Metallic service stairs and galleries on ‘Gaioleiro’ buildings (Andrade, 2011).

Ventilated masonry boxes on the ground floor prevented the rising moisture from the soil and the rotten of the interior wooden structures. These can be identified outside by metallic or masonry grids on the façade walls or on the entrance hall of the buildings with a first flight of masonry stairs that makes the connection to the interior timber staircase (Figure 12).

Figure 12 – First flight of masonry staircase gives access to an elevated ground floor with ventilated box underneath (Andrade, 2011 and Appleton, 2005).

4. DESCRIPTION OF THE STRUCTURE

In what concerns the foundation structure, the uptown soil is mostly composed by sandy-clay soils with low resistance rocks, thus buildings were commonly supported on caissons and arches structure (foundation soil more than three meters deep) or continuous walls in limestone masonry solid grounded (Figure 13). The foundation walls were usually larger below the façade walls, with 1.10 to 1.50 meters (m) thick, and thinner when below the side and light-shaft walls, around 0.60 m to 0.70 m thick (Appleton, 2003).

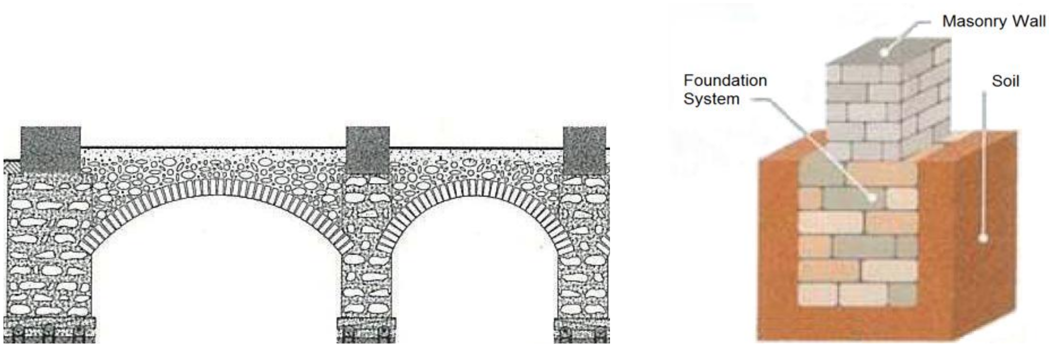

a) b)

Figure 13 - Foundation system: a) Caissons and arches structure (Silva, 2007); b) Continuous walls in limestone masonry (Appleton, 2003).

The exterior walls were built in rubble stone masonry linked by air lime mortar and sand (in a proportion of 2:1 - Figure 14). The front façade walls are typically 0.60 to 0.80 m thick on the ground floor, with a decreasing thickness with the elevation of the building, resulting in rooftop walls with 0.30 to 0.40 m of thickness (Lopes *et al*., 2008). The back façade walls were usually 0.50 to 0.60 m thick. By the end of the century, new industrial materials were introduced allowing different construction solutions. The light-shaft and side walls, originally built in rubble stone masonry, started to be replaced by bricks masonry walls (Figure 15). The wall thickness varies from 0.40 to 0.50 m in the case of the rubble stone masonry or 0.30 to 0.15 m with brick masonry, but often constant in height (Appleton, 2005).

a) b) c)

Figure 14 – Exterior Masonry Walls: a) Rubble composition of the masonry side wall (Andrade, 2011); b) Connection between façade and side wall; c) Reduction of the thickness along the height.

a) b)

Figure 15 – Brick masonry walls (Andrade, 2011): a) Example of a light-shaft with rubble stone masonry wall (on the left) and solid brick masonry wall (on the right); b) Hollow brick masonry wall.

With the exception of the 'Pombalino' buildings, old masonry buildings were built before the introduction of adequate seismic provisions (the first Portuguese modern code that enforces seismic design dates from 1958) and therefore, where based on empirical knowledge and on the available natural materials. The 'Pombalino' buildings were characterized by the design of a three-dimensional timber structure (named 'gaiola pombalina') formed by interior timber-masonry walls and timber floors, responsible for the bracing of the masonry exterior walls (Figure 16).

a) b) c)

Figure 16 – Timber structure characteristic of 'Pombalino' buildings: a) global model of a building (Silva, 2007); b) vertical and horizontal timber struts reinforced the masonry walls around door and window openings (Appleton, 2008); c) 'Frontal' walls (Appleton, 2008).

This wood structure results on the buildings strength and energy dissipation capacity, essential to support the seismic actions in any direction (Lopes, 2010). Nevertheless, with the construction of 'Gaioleiro' buildings this constructive method was gradually abandoned resulting on the design of buildings with inferior constructive quality. In fact, the name 'Gaioleiro' is connected with the 'gaiola pombalina' structure in a depreciatory way.

The timber structure from the 'frontal' walls started to be simplified (with the elimination of the diagonal elements) and the rubble masonry infill replaced by masonry bricks (solid or hollow). The thickness of the brick masonry walls decreases along the height of the building by changing the position of the bricks (Figure 17). This variation is also related with the transition between solid masonry bricks on the lower floors and hollow bricks on the upper floors or the replacement of the brick masonry walls by 'tabique' walls (Figure 18). These 'tabique' walls were made of timber laths nailed to vertical joists, filled afterwards by rubble masonry and mortar. These walls have a deformable and light structure and were originally used as partition walls. However, in 'Gaioleiro' buildings 'tabique' walls assume a structural role as they were copiously used on the superior floors of the buildings.

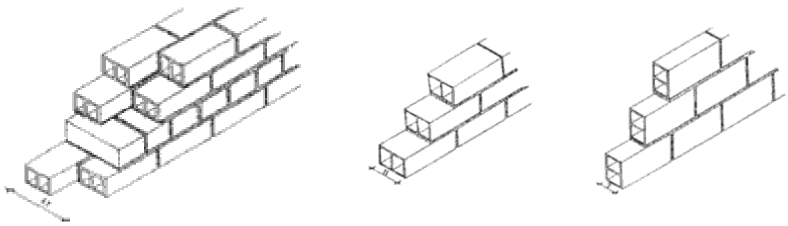

Figure 17 – Brick masonry walls.

a) b) c)

Figure 18 – Interior structure characteristic of 'Gaioleiro' buildings: a) hollow brick wall; b) solid brick wall (Andrade, 2011); and b) 'tabique' walls (Pena, 2008).

The floors were composed by wooden beams with 0.07 to 0.08 m width and 0.16 to 0.22 m height disposed 0.35 to 0.40 m apart, placed perpendicular to the façade walls and usually braced by smaller beams that prevent the transverse deformation of the main beams (Figure 19 a). The floors were made of soft pine strips with 0.15 m large arranged perpendicular to the main wooden beams (Figure 19 b). The ceilings were finished by wooden strips covered with plaster and interesting stucco details (Figure 19 c and d).

a) b) c) d)

Figure 19 – Floor structure: a) Excessive deformation of a timber beams where apparently no locking joist were use; b) Ceiling finished with laths and plaster (Branco, 2007); c) and d) Examples of ceiling covered by stucco details and frames (Andrade, 2011).

The connections between walls (interior and exterior) and between walls and floors are probably one of the main weaknesses of these buildings when subjected to seismic actions. Other structural limitations are related with variation of the interior structure with the height of the building, along with the increasing number of storeys and high ceiling heights. As a result, the masonry walls are not continuously supported by the interior structure and are, therefore, prone to out-of-plane failure. Actually, there is the record of a number of buildings that collapsed even during the construction process (Figure 20).

Figure 20 – Collapse of 'Gaioleiro' buildings (Lopes *et al*., 2008).

As to the floors, the spans also become more generous, leading to increasing deformations and consequent degradation of ceilings. The weak connections between the floor beams and the masonry walls and the lack of nailing fixation between the beams and the floor boards result on the low horizontal stiffness of the floors. This feature is a major disadvantage as it influences the transmission of horizontal seismic actions (as inertial forces) to the resistant structure. Moreover, these buildings have a rectangular shape in plan, generating structures with disproportional dimensions and distinct behaviour when subjected to directional dynamic actions.

The balconies and galleries from the back façade walls were built with iron beams in shape of I or T profile (around 0.20 m height) and brick masonry disposed in vaults, interconnected by air lime mortar or cement (Figure 21). The floors were restrained by the side and back masonry walls and supported on border beams and slender circular columns (Figure 22 a). Occasionally, there are diagonal tie rods connecting the border beams to the façade walls, supporting balconies which can reach 2.5 m depth. The service staircases were made of circular metallic columns, braced by I or T profile beams which was the support to the stairs made of metallic grid plates (Figure 22 b). The columns were founded on masonry sabots, while the stairs levels were embedded on the balconies' beams.

Figure 21 - Floors made of metallic beams and ceramic bricks interconnected by mortar or cement (Appleton, 2005).

a) b) c)

Figure 22 – Back façade wall: a) Metallic balconies supported by slender columns (Appleton, 2005); b) Metallic service staircase; c) Interior backyard.

The age of the buildings combined with the lack of proper maintenance actions affect the durability and the resistance of the structural materials. Therefore, the assessment of the seismic vulnerability of masonry buildings must be supported on their chronologic evolution, including the survey of the structural modifications performed and causes of degradation. Annex A summarizes the main features of this typology of masonry buildings.

On one hand, the age of the buildings combined with a reduced maintenance and consequent degradation, support the concern about their structural safety. On the other hand, existing buildings have been subjected to significant structural modifications, diluting their original design. The analyses may also take into account the structural interaction between buildings, as they were frequently built in compounds sharing the side rubble masonry walls. The structural interventions and retrofitting measures should be taken in a global perspective, which would possibly result in a more sustainable rehabilitation of the building stock.

5. REVIEW OF CASE STUDIES OF ‘GAIOLEIRO’ BUILDINGS

The increasing concern about the built heritage led to the development of several studies regarding the assessment of structural performance and seismic vulnerability of old masonry buildings. However, there are still few works regarding the ‘Gaioleiro’ buildings constructive system. Annex B resumes the main features of the studies listed in this section, while Annex C summarizes the mechanical properties of the structural materials considered in this works.

Costa and Oliveira (1989) assessed the seismic behaviour of a ‘Gaioleiro’ quarter of buildings, near to D. Afonso Henriques Alley. In 1996, Lopes and Azevedo performed some in-situ tests on a ‘Gaioleiro’ building in Alcântara which was to be demolished (Lopes and Azevedo, 1997). The tests were performed in three interior ‘tabique’ walls, one brick masonry walls from the staircase and one exterior masonry wall (Figure 23).

Figure 23 – In-situ test in masonry wall, including some instrumental details (Lopes, 2010).

On the façade walls experimental test, the panel was divided in two and the largest one was used as a reaction support so that the horizontal actions applied by the hydraulic jacks were high enough to bring the tested wall to collapse. The tests were performed with monotonic loading. With the experimental results, a simplified numerical model of the building was developed. At the end, it was clear the high seismic vulnerability of the building (Lopes and Azevedo, 1997). It was estimated that the building had about 43% of the necessary strength to support the seismic design action, as defined in RSA (1983).

In 2001, Appleton developed a survey about a quarter in ‘Avenidas Novas’ built between 1908 and 1930. The buildings were analysed in terms of their current functional requirements and at the end, an intervention methodology was defined in order to update ‘Gaioleiro’ buildings according to new standards of security, habitability, use, economy and image.

Then, in 2003, Branco and Correia performed an experimental campaign over brick masonry walls from the Campo Pequeno Bullring built in 1892. This experiment allowed the determination of the compression strength of the panels (Figure 24), which are expected to be similar to those used on the ‘Gaioleiro’ residential buildings.

Figure 24 – Frame for monotonic compression test on masonry panel from Campo Pequeno Bullring (Branco and Correia, 2003).

Branco (2007) analysed the feasibility of some rehabilitation techniques on ‘Gaioleiro’ buildings, namely the implementation of reinforced concrete walls on the light-shafts, the adaptation of a base isolation system and the use of viscous dampers. The study considered a three dimensional numerical model representative of an existing ‘Gaioleiro’ building (Figure 25) based on Finite Elements Method, making use of the software SAP2000® (Figure 26).

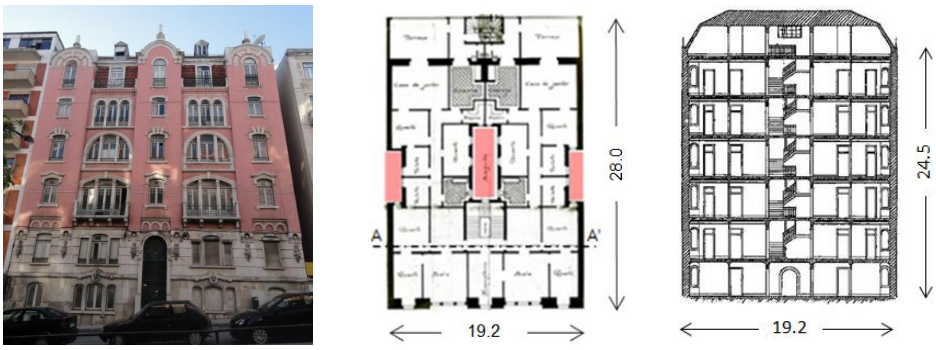

a) b) c)

Figure 25 – ‘Gaioleiro’ building located on Duque de Loulé Avenue (Branco, 2007): a) Façade wall; b) Plan of a current floor; c) Cross section A-A’.

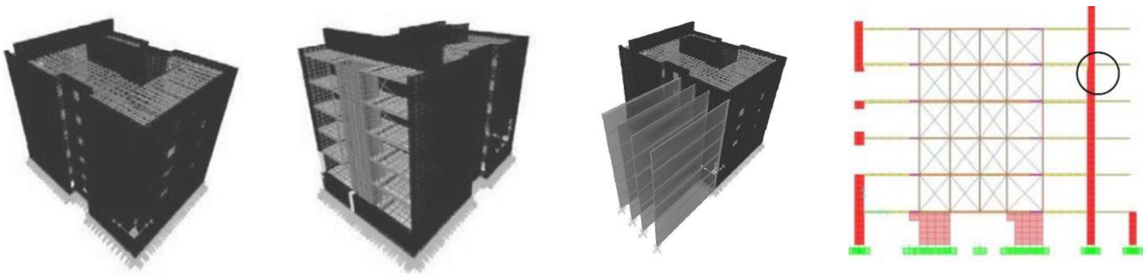

a) b) c) d)

Figure 26 - Numerical Model (Branco, 2007): a) Global model of the building; b) Back façade wall with the ceramic brick balconies; c) Final model taking into account the adjacent reinforced concrete building; d) Cross section of the building with the reduction of the masonry wall thickness between the 4th and the 5th floor.

The building is composed by a basement, five storeys high and mansard roof and is made by rubble stone masonry exterior walls and interior timber floors and roof. The interior walls parallel to the façade walls are made of hollow brick masonry, while the remaining interior walls are made of 'tabique'. However, on the last floor all the interior walls are made of 'tabique'. The building has three light-shafts, one on the centre of the building and two adjacent to the side walls (Figure 25 b). The left side wall is close to a reinforced concrete structure, while the right side wall is next to a pedestrian access. Table 1 summarizes the main mechanical and geometrical properties of the materials.

Table 1 – Mechanical and Geometrical properties of the building.

Structural Material	**Mechanical Properties**	**Structural Element**	**Dimension**
Rubble Stone Masonry	γ = 22.0 kN/m^3 E_i ([1]) = 3000 MPa E_f ([1]) = 1000 MPa ν = 0.2 ξ = 5%	Front Façade Wall	0.90 m (<4th floor) 0.80 m (> 4th floor)
		Back Façade Wall Side Walls	0.60 m (<4th floor) 0.50 m (>4th floor)
	f_c = 4.00 MPa ([2]) f_t = - 0.40 MPa ([2]) τ = 0.14 MPa ([2])	Central Light-Shaft Walls	0.40 m
		Lateral Light-Shaft Walls	0.50 m
Hollow Brick Masonry([3])	γ = 14.6 kN/m^3 E_i ([1]) = 1000 MPa E_f ([1]) = 500 MPa ν = 0.2 ξ = 5%	Staircase Walls (Back Façade Wall)	0.30 m
		Interior Walls (Basement)	
'Tabique' Wall	Square strips nailed to vertical 0.15 m stripes filled on the breaks by rubble masonry	Interior Walls	0.10 m
Pine Wood	γ = 6 kN/m^3 E = 6000 MPa ν = 0.2 ξ = 5%	Main Beams	0.18 x 0.08 m^2 0.40 m apart
		Secondary Beams	0.08 x 0.08 m^2

In the numerical model, the rubble exterior masonry walls were simulated through volume elements. This option was taken because it allowed the consideration of a more realistic distortion of the elements and the visualization of the stress distribution on the wall and along the thickness of the wall (Branco, 2007). The walls were modelled with two layers of solid elements in order to reproduce the reduction of the wall thickness along the height of the building (Figure 26 d). This conclusion resulted from the comparison between the analyses of model with volume elements and with shell elements on the masonry exterior walls.

[1] The Young's Modulus (E) was determined by calibration of the numerical model with the results of the in-situ dynamic characterization tests.
[2] Results from Costa and Oliveira (1989).
[3] The available results are referred to solid brick masonry (Branco and Correia, 2003).

Shell elements were used to simulate the brick masonry walls from the basement and from the back façade staircase. The weight of the rubble and brick masonry walls was defined on the materials properties.

Frame elements were adopted to model the ‘tabique’ walls and the floor beams, since the rigid diaphragm assumption is not admissible. The ‘tabique’ walls were modelled through a frame structure braced by two diagonal joists. The determination of the elements section was based on the results from the shear failure tests performed on ‘tabique’ walls by Lopes and Azevedo (1997 - Figure 27).

The option of modelling the partition walls resulted from the need to ensure the support of the floors and to create lateral support to the exterior masonry walls. These elements also connect the exterior walls to the interior light-shaft walls increasing the horizontal stiffness of the building. The weight of the interior ‘tabique’ walls was uniform distributed on the floors in order to minimize local vibration modes on the vertical non-resistant elements.

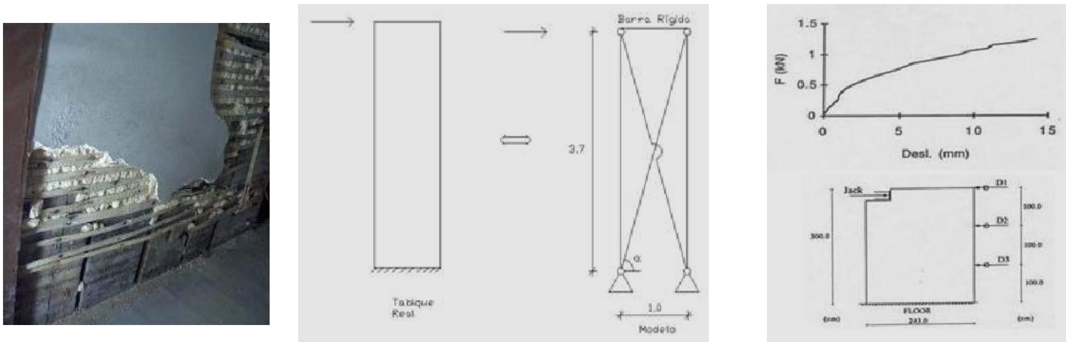

a) b) c)

Figure 27 – Numerical Model of ‘tabique’ walls (Branco, 2007): a) ‘Tabique’ wall (Pena, 2008); b) Model of the ‘tabique’ walls; c) Results from the shear test over ‘tabique’ wall (Lopes and Azevedo, 1997).

The timber floors are composed by main beams supported on the façade walls and on the central light-shaft walls, locked on the perpendicular direction by secondary beams. The floor was modelled by a grid of frame elements, taking into account the spacing between the structural elements on numerical model and their actual distribution. To avoid the creation of several frame elements with different spacing between, the frame elements were defined with constant properties (section and spacing) allowing the correction of the Moment of Inertia according to each set of spacing considered on the model (Figure 28).

$$\text{Inertia Correction Factor} = \frac{I_x \times d}{I'_x}$$

$$\text{Equivalent Density} = \frac{d \times W}{A}$$

I_x – Moment of Inertia (per meter)
I_x' – Moment of Inertia of a beam
d – Spacing between beams
W – Uniform Weight
A – Cross Section Area

Figure 28 – Modelling of the timber floors (Branco, 2007).

Even though this correction factor is not suitable for the perpendicular direction of the main beams (Y), the moment of inertia is also less important for the analysis. Thus, the inertia correction factor approximation was also used. The weight of the timber floors also took into account an equivalent density for each set of spacing (Figure 28), and was defined uniform distributed on the floor level.

The balconies of the back façade wall are made of iron beams in shape of I or T profile (around 0.20 m height) and brick masonry disposed in vaults, interconnected by air lime mortar or cement. It was assumed that these balconies were close to the behaviour of a reinforced concrete slab. This simplification is also due to the limited relevance of this structure to the overall behaviour of the building. The weight of the back balconies and roof structure were defined uniform distributed on the floor level.

Table 2 summarizes the finite elements used on the numerical model of the building.

Table 2 – Finite Elements used on the numerical model.

Finite Element	Modelling	Observations
Volume (8 joints)	Exterior Masonry Walls (Rubble Stone Masonry)	– The distortion deformation of the volume elements is closer to the behaviour of masonry walls; – Visualization of the stress distribution on the wall and along the thickness of the wall; – The weight was defined on the materials properties.
Shell (4 joints) Membrane and plate behaviour	Basement Interior Walls Back Staircase Walls (Brick Masonry Walls)	– The weight was defined on the materials properties.
	Back Balconies Floor (Iron beams and brick masonry)	– Behaviour close to a reinforced concrete slab; – The weight was defined uniform distributed on the floor level.
Frame (2 joints) Beam-Colum behaviour	'Tabique' Walls	– The partition walls were modelled to ensure the support of the floors and to create some lateral locking to the exterior masonry walls; – Frame structure braced by two diagonal joists; – The frame section was based on the results from the shear failure tests performed on 'tabique' walls (Lopes and Azevedo 1997); – The weight was uniform distributed on the floors in order to minimize local vibration modes on the vertical non-resistant elements.
	Timber Floor	– Grid of frame elements taking into account the spacing between the structural elements on numerical model and their actual distribution; – The weight also considered an equivalent density for each set of spacing and was defined uniform distributed on the floor level.

The model was tested and calibrated based on in-situ dynamic characterization tests. This procedure revealed the importance of taking into account the influence of the adjacent reinforced concrete building, considered in the model through the introduction of vertical walls perpendicular to the side walls of the 'Gaioleiro' building (shell elements - Figure 26 c). At the end of the analyses, the rehabilitation techniques lead to a better seismic behaviour of the building, namely related to an increase of the structural stiffness (concrete walls), reduction of displacements between floor levels (base isolation) and with an increase of the energy dissipation (viscous dampers).

In 2007, another 'Gaioleiro' building was simulated by a three dimensional model based on Finite Elements Method, making use of the software SAP2000® (Jesus, 2007 - Figure 29). The study aims the assessment of the seismic behaviour of the building structure taking into account different enhancement factors for the seismic action (according with RSA, 1983). At the end, the building was strengthened by reinforced plaster incorporating a steel mesh, and again analysed taking into account different enhancement factors for the seismic action.

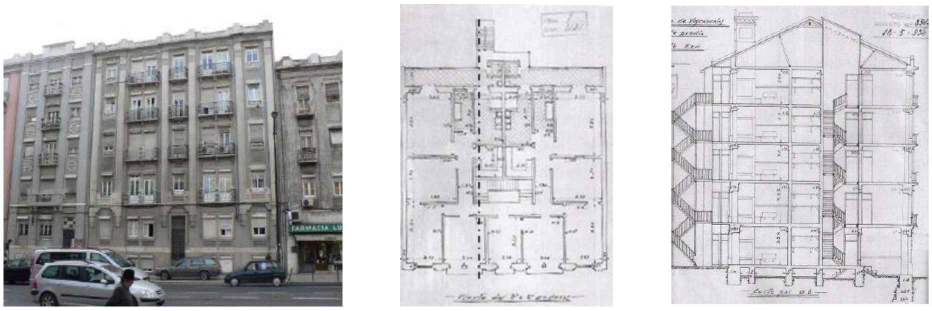

a) b) c)

Figure 29 – 'Gaioleiro' building located at Almirante Reis Avenue (Jesus, 2007): a) Front façade wall; b) Plan of a current floor; c) Longitudinal cross section.

The building is composed with five storeys and is made of rubble masonry exterior walls, interior brick masonry walls and timber floors and roof. The construction belongs to a compound of buildings, possibly sharing the side walls with the adjacent buildings. Table 3 summarizes the main mechanical and geometrical properties of the structural materials and elements of the building. It was assumed that the quality of the masonry work on the side walls is weaker than the masonry façade walls, exception made to the walls from the ground floor level (Figure 30 c).

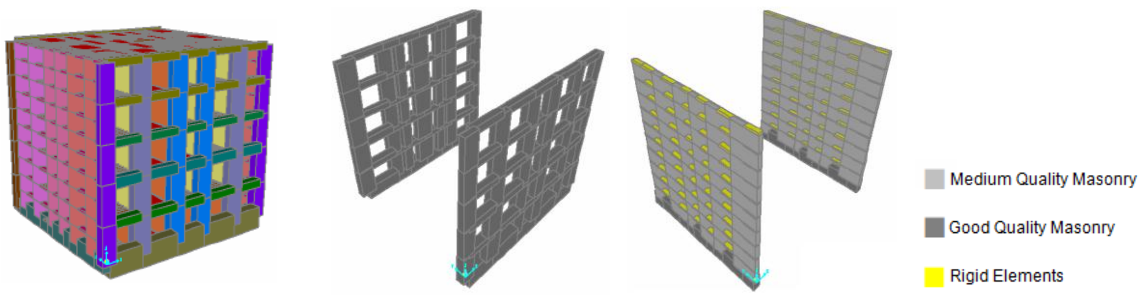

a) b) c)

Figure 30 - Numerical Model (Jesus, 2007): a) Global model of the building; b) Model of the façade walls; c) Model of the gable walls (rigid elements).

Table 3 - Mechanical and Geometrical Properties of the building.

<table>
<tr><th>Structural Material</th><th colspan="2">Mechanical Properties</th><th>Structural Element</th><th colspan="2">Dimension</th></tr>
<tr><td rowspan="7">Rubble Stone Masonry</td><td rowspan="5">Good Quality Masonry Wall</td><td rowspan="3">γ = 22.0 kN/m^3
E_i (4) = 2000 MPa
E_f (4) = 4000 MPa
ν = 0.2</td><td rowspan="5">Façade Wall</td><td>Ground Floor</td><td>0.80 m</td></tr>
<tr><td>1st Storey</td><td>0.70 m</td></tr>
<tr><td>2nd Storey</td><td>0.60 m</td></tr>
<tr><td rowspan="2">f_c = 8.0 MPa
f_t = - 0.20 MPa
τ = 0.40 MPa</td><td>3rd Storey</td><td>0.50 m</td></tr>
<tr><td>4th Storey</td><td>0.50 m</td></tr>
<tr><td rowspan="2">Medium Quality Masonry Wall</td><td>γ = 22.0 kN/m^3
E = 600 MPa
ν = 0.2</td><td rowspan="2">Side Walls</td><td>Ground Floor – 1st Storey</td><td>0.45 m</td></tr>
<tr><td>f_c = 0.90 MPa
f_t = - 0.10 MPa
τ = 0.10 MPa</td><td>2nd Storey – 4th Storey</td><td>0.40 m</td></tr>
<tr><td rowspan="5">Solid Brick Masonry</td><td rowspan="3">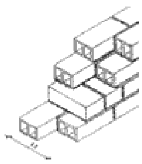</td><td rowspan="2">γ = 3.75 kN/m^3
E_i (4) = 1000 MPa
E_f (4) = 3200 MPa
ν = 0.2</td><td>Interior Walls from the ground floor</td><td colspan="2" rowspan="3">0.25 m</td></tr>
<tr><td>1st and 2nd storey walls parallel to the façade walls</td></tr>
<tr><td>f_c = 5.00 MPa
f_t = - 0.10 MPa
τ = 0.20 MPa</td><td>Staircase Walls</td></tr>
<tr><td rowspan="2">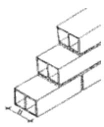</td><td>γ = 2.10 kN/m^3
E_i (4) = 1000 MPa
E_f (4) = 3200 MPa
ν = 0.2</td><td>1st and 2nd storey walls perpendicular to the façade walls</td><td colspan="2" rowspan="2">0.15 m</td></tr>
<tr><td>f_c = 5.00 MPa
f_t = - 0.10 MPa
τ = 0.20 MPa</td><td>3rd and 4th storey walls</td></tr>
<tr><td rowspan="2">Pine Wood</td><td colspan="2" rowspan="2">E = 8000 MPa
ν = 0.2</td><td>Main Beams</td><td colspan="2">0.18 x 0.08 m^2
0.40 m apart</td></tr>
<tr><td>Secondary Beams</td><td colspan="2">0.18 x 0.08 m^2</td></tr>
</table>

The structural elements were modelled by frame elements with the equivalent geometrical characteristics of the building structure. The façade walls were discretized in vertical elements (piers) and horizontal elements (spandrels) around the façade openings. The piers were modelled by vertical frames (columns) and the spandrels were modelled by horizontal frames (beams) (Figure 31). The side walls were modelled by several vertical frame elements, connected by horizontal rigid elements (high axial and bending stiffness) at the floor level to guarantee the compatibility between the elements (Jesus, 2007 - Figure 31).

4 The modulus of elasticity (E) was determined by calibration of the numerical model with the results of the in-situ dynamic characterization tests.

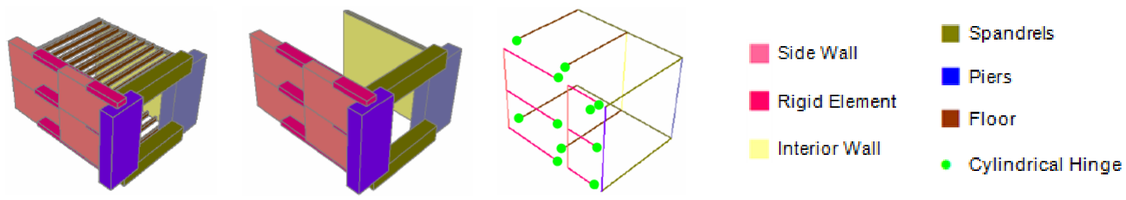

a) b) c)

Figure 31 – Numerical Model (Jesus, 2007): a) Floor beams; b) Interior Wall; c) Frame Elements.

The timber floors are composed by main beams supported on the façade walls and on the parallel interior walls and locked on the perpendicular direction by secondary beams. The floor beams were modelled through bi-articulated frames simulating therefore the flexibility of the floors. The timber stairs were also modelled by bi-articulated frame elements to restrain the transmission of moments to the stairs.

The balconies of the back façade wall are made of iron beams in shape of I or T profile (around 0.20 m height) and brick masonry disposed in vaults, interconnected by air lime mortar or cement. These structures were defined through distributed loads on the back façade wall, while the timber roof structure was defined by a uniform distributed load on the floor level.

Table 4 summarizes the finite elements used on the numerical model of the building. The model was tested and calibrated based on in-situ dynamic characterization tests.

Table 4 - Finite Elements used on the numerical model.

<table>
<tr><th>Finite Element</th><th>Modelling</th><th>Observations</th></tr>
<tr><td rowspan="4">Frame
(2 joints)

Beam-Column behaviour</td><td>Façade Masonry Walls</td><td>– Vertical frame elements modelling the piers;
– Horizontal frame elements modelling the spandrels;
– The weight was defined on materials properties.</td></tr>
<tr><td>Side Masonry Walls</td><td>– Several vertical frame elements connected by horizontal rigid elements at the floor level to guarantee the compatibility between the vertical frame elements;
– The weight was defined on the materials properties.</td></tr>
<tr><td>Interior Brick Masonry Walls</td><td>– The weight was defined on the materials properties.</td></tr>
<tr><td>Timber Floor and Stairs</td><td>– The beams were modelled through a grid o bi-articulated frames;
– The weight was defined distributed at the floor level.</td></tr>
</table>

In 2008, an experimental campaign was developed on 'Laboratório Nacional de Engenharia Civil' (LNEC – National Laboratory of Civil Engineering in Lisbon) considering the seismic vulnerability of the 'Gaioleiro' typology of buildings (Candeias, 2008). Five prototypes were built in a reduced scale (1:3) and tested on the LNEC tri-axial shaking table to assess the seismic behaviour of the masonry buildings (Figure 32) and assess the effect of three different reinforcement solutions, represented in Figure 33.

Figure 32 – Overview of the building prototype before test and test setup (Candeias, 2008).

The prototypes have four storeys high and are composed by exterior masonry walls, with openings in two opposite walls, and timber floors. The exterior walls were built by a self-compacting bentonite-lime concrete, specially made to simulate the behaviour of the original rubble masonry walls. The floors were made of timber beams parallel to the façade walls (smaller dimension in plan of the building) and medium-density fibreboard (MDF) panels stapled to the floor beams to simulate flexible floors with very limited diaphragmatic action.

Nonetheless, the prototypes do not consider the reduction of the walls thickness in high, the interior walls, the floor boards or the mass concentration on the floor level, or the structural interaction between buildings, several features which might compromise the global structural behaviour (Candeias, 2008). Table 5 summarizes the main mechanical and geometrical properties of the structural materials and elements of the building.

Table 5 - Mechanical and Geometrical Properties of the building.

Structural Material	**Mechanical Properties**	**Structural Element**	**Dimension (reduced scale 1:3)**
Self-compacting bentonite-lime concrete	γ = 19.10 kN/m^3 E = 750 MPa υ = 0.20	Façade and Side Walls	0.15 m
	f_c = 0.70 MPa		
Pine Wood	γ = 5.80 kN/m^3 E = 12000 MPa	Main Beams	0.10 x 0.075 m^2 0.25 m apart
		Ring Beams	0.30 x 0.075 m^2
MDF Panels	γ = 7.60 kN/m^3 E = 120 MPa	Floor Boards	0.57 x 1.05 x 0.012 m^3

The unreinforced prototypes aim to simulate the floors flexibility, the behaviour of the connections between walls and floors and the consequences of the façade openings to the seismic behaviour of these buildings (Model 0). The first reinforced prototype was intended to avoid the collapse of façade walls due to out-of-plane displacements (Model 1 - Figure 33 a). The second reinforced prototype aimed to improve the wall behaviour in its plane through the connection of opposite walls by metallic rods at the floor level (Model 2 - Figure 33 b). The third solution aimed to control generalized cracking on the façade walls related to the low tensile strength of the masonry (Model 3 - Figure 33 c).

Model 1

Model 2

Model 3

Figure 33 - Description of the reinforcement solutions (Candeias, 2008): Model 1 - Introduction of metallic connections between masonry walls and floors and fibreglass strips linked with epoxy resins on the front and back façade walls of the 3rd and 4th storey; Model 2 - Connection of opposite masonry walls by tie rods at the floor level; Model 3 - Introduction of fibreglass strips linked with epoxy resins on the front and back façade wall.

The dynamic tests were performed on the LNEC shaking table by imposing time series of artificial accelerograms compatible with the design response spectrum defined by the Portuguese Code RSA (1983). The time series were imposed with increasing amplitude (PGA) and in two uncorrelated orthogonal directions (Figure 33 – Test Setup). Before the beginning of the tests and after each time series, the dynamic properties of the models were characterized.

The damage pattern observed during the experimental tests revealed that the seismic behaviour of the models is very much affected by the type of strengthening solution. The two unreinforced prototypes and the second strengthening solution (Model 2 - Figure 33) were after modelled with simplified numerical models based on macro-elements. Linear static and nonlinear analyses were performed and calibrated with the experimental results obtained (Candeias, 2008). Comparing the capacity curves of the analysed prototypes, it is possible to conclude that seismic resistance of the models did not significantly improved. However, there is a slight improvement in the energy dissipation capacity and significant improvements on the control of out-of-plane displacements.

After, Salvado (2009) analysed two different numerical models (Salvado, 2009) based on the damage distribution of the unreinforced prototype (Model 0 - Figure 34). Firstly, five three dimensional numerical model were developed based on Finite Elements Method, making use of the software SAP2000® (Figure 34 a) to simulate the consecutive experiments performed with the prototype (Candeias, 2008). Linear dynamic analysis were performed in each numerical model and completed with the successive adjustment of the mechanical properties of the masonry (modulus of elasticity) zone by zone, in order to simulate the damage observed on the experimental model.

The previous Table 5 summarizes the main mechanical and geometrical properties of the structural materials and elements of the building, exception made to the self-compacting bentonite-lime concrete (exterior walls) modulus of elasticity from the first numerical model, which had to be adjusted to be consistent with the frequencies and modal shapes obtained from the experimental test. On the following numerical models, the modulus of elasticity was adjusted taking into account the local stiffness decreasing in result of cracking pattern. Table 6 summarizes the finite elements used on the global numerical model of the building. The vertical finite elements were simply supported on the ground foundation, accounting the restrain of the three translational displacements and the release of the rotations. It was considered that most of the foundation settlements have already occurred and because, on the other hand, the foundation soil has good features.

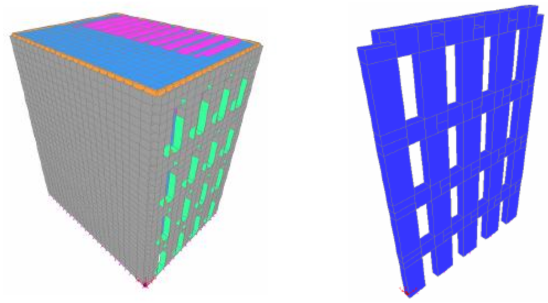

a) b)

Figure 34 - Numerical Model (Salvado, 2009): a) Three dimensional finite model of the building; b) Simplified macro-element model of the façade wall.

Table 6 – Finite Elements used on the global numerical model.

Finite Element	**Modelling**	**Observations**
Shell (4 joints) Membrane and plate behaviour	Façade and Side Walls	– The weight was defined on the materials properties.
	Floor Boards	– Grid of shell elements with an average area of 0.15 x 0.15 m^2 per element; – The shell elements are simply supported on the floor beams accounting the restrain of the three translation degrees of freedom (xx, yy, zz) and the release of the three rotations degrees of freedom (xx, yy, zz); – The weight was defined distributed at the floor level.
Frame (2 joints) Beam-Column behaviour	Floor Beams	– The end of the beams are supported on the ring beams and accounts the release of two rotations degrees of freedom (xx and yy); – The weight was defined distributed at the floor level.
	Ring Beams	– The ring beams are built-in support the masonry walls; – The connection between perpendicular ring beams accounts the release of two rotations degrees of freedom (xx and yy); – The weight was defined distributed at the floor level.

The building façade wall was then represented by a simplified numerical model based on the equivalent frame method (macro-elements), making use of the software SAP2000® (Figure 34 b). This new model was used to perform a nonlinear static analysis to estimate the capacity curve (pushover curve) of the façade wall in its plane. The nonlinear behaviour of the masonry was represented by plastic hinges taking into account the possible failure mechanisms of this type of buildings. Table 7 summarizes the main mechanical and geometrical properties of the masonry used on the simplified model and Table 8 summarizes the modelling hypothesis.

Table 7 - Mechanical properties of the rubble masonry used on the simplified model.

Structural Material	**Mechanical Properties**		**Dimension (reduced scale 1:3)**
Self-compacting bentonite-lime concrete	γ = 19.10 kN/m^3 E = 750 MPa G = 250 MPa	f_c = 1.00 MPa τ = 0.125 MPa	0.15 m

Table 8 – Macro-Elements used on the simplified numerical model.

Macro-Element	**Modelling**	**Observations**
Plastic Hinges	Piers	– One bending hinge at the end of the ground piers (to simulate the connection to the ground foundation); – One shear hinge at mid height.
	Spandrels	– One shear hinge at mid height.

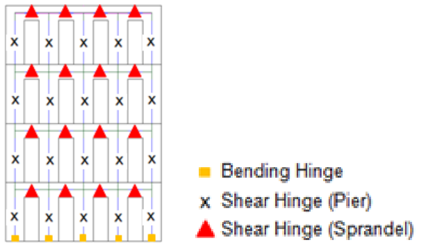

On the masonry façade wall each pier and spandrel may be divided into three distinct sections. At both ends of the elements there are two pieces of rigid masonry, corresponding to the zone located outside the doors in the front side of the building, and a deformable section located between the two rigid sections, corresponding to the zone located on the façade doors. Therefore, the masonry elements were modelled by introducing one bending hinge at the end of the ground piers (to simulate the connection to the ground foundation) and one shear hinge at mid height of each spandrel and pier.

This assumption results from the observation of the experimental tests performed (Candeias, 2008), where it appears that the façade wall collapse was due to shear failure at mid span of spandrels (sliding shear) and, in addition there was no rocking failure at any pier. The numerical analysis is close to the experimental tests in terms of collapse mechanism and in terms of ultimate force and displacement.

Finally a performance based seismic assessment of the façade wall was carried out, concluding that this structure reaches the criteria of acceptability for an occasional earthquake, as well as both rare and very rare earthquakes. As the study was performed on façade wall plan, nothing can be concluded regarding the performance of the three dimensional of the building or about the out of plane behaviour of the façade wall.

The results from this study show that the continuous three dimensional model, with which consecutive linear dynamic analysis were performed, can very reasonably reproduce the experimental tests. However, for higher seismic actions, the numerical and experimental results are slightly different due to the linear nature of the numerical analysis. The macro-element model successfully reproduced the façade wall behaviour on its plane, confirming the adjustment and applicability of such numerical models.

Mendes and Lourenço (2009) developed the numerical model of the unreinforced prototype (Model 0) and of the first strengthening solution (Model 1 - Figure 33) using the Finite Element software DIANA® (Figure 35). The modelling hypothesis adopted were similar to the ones considered by Salvado (2009), summarized in Table 6.

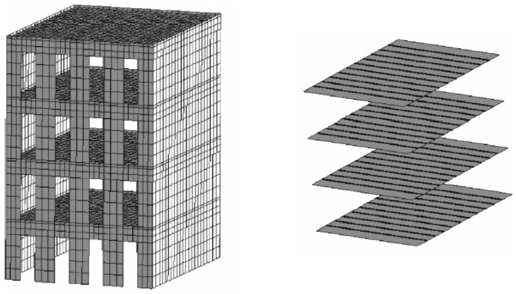

a) b)

Figure 35 – Numerical Model (Mendes and Lourenço, 2009): a) Global view of the building; b) Floor elements.

The exterior masonry walls were simulated through shell elements, while the floor beams were simulated through frame elements. Shell elements were also used on the floors in order to simulate the in-plane deformability. On the connection between the building and the ground foundation, only the translation degrees of freedom in the base were restrained.

The behaviour of the connection between the floors and the walls is unknown, as, during the experimental tests, no measurements were taken for a possible separation of the elements and the eigenmodes in the longitudinal direction (parallel to the side walls) were difficult to characterize due to the presence of noise (Mendes and Lourenço, 2009). Therefore, preliminary numerical analyses were carried out with the purpose of validating the assumption used for the floor-wall connection and of obtaining a crack pattern similar to the one obtained in the tests.

It was noted that the behaviour of Model 0 and Model 1 were similar for low acceleration amplitudes, where the response of the prototypes was basically linear elastic, while under the higher acceleration amplitudes the prototypes presented nonlinear behaviour. On the numerical model, the nonlinear behaviour of the masonry walls was simulated using the Total Strain Cracking Model detailed in software DIANA®.

Reasonable nonlinear properties were initially assumed for the masonry material with successive adjustments in the fracture energies (G_i). The masonry behaviour was simulated by a parabolic stress-strain relation for compression and an exponential tension-softening relation for tension (Figure 36). For the shear behaviour was adopted a constant retention factor. The damping (C) was simulated according to Rayleigh viscous damping and determined from the results obtained in the dynamic identification tests. The iterative calibration process result on the adjustment of the modulus of elasticity of the exterior walls (E = 779 MPa) and of the MDF Panels (E = 240 MPa). Table 9 summarizes the values adopted.

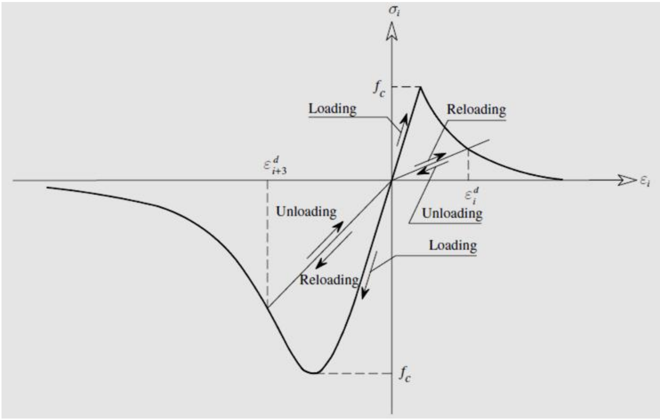

Figure 36 – Adopted hysteretic behaviour of masonry (Mendes and Lourenço, 2009).

Table 9 – Nonlinear behaviour of masonry walls.

Structural Material	**Mechanical Properties**		**Modelling Hypothesis**
Self-compacting bentonite-lime concrete	γ = 19.10 kN/m^3 E = 779 MPa υ = 0.2	f_c = 0.80 MPa G_c = 1.25 N/mm	− Compression behaviour simulated by a parabolic stress-strain relation.
		f_t = 0.125 MPa G_t = 0.125 N/mm	− Tensile behaviour simulated by an exponential tension-softening relation.
		β = 0.01	− Shear behaviour simulated by a constant retention factor.

After the calibration of the numerical models, it was concluded that the hypothesis of a full translation wall-floor connection was the most appropriate solution with the observed experimental model results (Mendes and Lourenço, 2009).

With the incorporation of the code loads on the calibrated numerical model (partition walls, cladding and roof) a safety analysis was performed making use of a nonlinear time history analysis and nonlinear static analysis.

With the nonlinear time history analysis it was observed that the building with appropriate floor-wall connection (Model 1) was in the limit of its loading capacity when subjected to the seismic action proposed in the EC8 National Annex. Therefore, it seems that a strong floor-wall connection is not enough to guarantee the good performance of the building under seismic load.

In the nonlinear static analysis the capacity curve of the building was considered by increasing a set of lateral loads, applied to the structure in two independent directions. With respect to the nonlinear static analysis proportional to the mass or to the 1st mode, it was concluded that these do not simulate correctly the damage of the structure.

It became clear that the vibration modes with higher frequencies had a significant contribution to the behaviour of the building. Thus, an adaptive nonlinear static analysis was, in addition, performed. In this case, the load distribution was updated as a function of the existing damage. At the end, this analysis did not provide any improvement in terms of load-displacement diagrams or failure mechanisms. The flexible floors are most likely the reason for the deficient performance of the nonlinear static analysis (Mendes and Lourenço, 2009).

In 2011, Andrade developed a review about the construction techniques, material properties and structural behaviour of 'Gaioleiro' buildings (Andrade, 2011). The purpose of the study was to obtain a specific description of the characteristics of this typology of buildings helpful for future interventions. Gomes (2011), studied in detail the architecture, the construction and the structure of three existing 'Gaioleiro' buildings, supporting the available bibliographic information on the subject.

7. CONCLUSION

This paper presents a brief description of the masonry 'Gaioleiro' buildings characteristic of the urban expansion of Lisbon at the end of the nineteenth century and after the 'Pombalino' reconstruction. The exterior walls were made of rubble stone masonry linked by air lime mortar and sand, with a decreasing thickness with the height of the buildings. The side walls are interrupted by light-shafts providing natural light and ventilation to the interior rooms.

The interior timber cage structure characteristic of the preceding 'Pombalino' buildings was progressively replaced by brick masonry walls and 'tabique' walls. Nonetheless, the interior structure is very variable considering the transition between solid masonry bricks on the lower floors and hollow bricks on the upper floors or the replacement of the brick masonry walls by 'tabique' walls. The floors were made by wooden beams, usually placed perpendicular to the façade walls, and embedded on the masonry. Nevertheless, the weak connections to the masonry walls and the lack of nailing fixation between the beams and the floor boards result on the low horizontal stiffness of the pavements.

The connections between walls and between walls and pavements are probably one of the main weaknesses of these buildings when subjected to seismic actions. Other structural limitations are related with the increasing number of floors and high ceiling heights. Conversely, the masonry walls are not laterally supported by the interior structure and, are therefore prone to out-of-plane failure. The age of the buildings combined with the lack of proper maintenance work and the posterior structural interventions performed on the buildings affects the durability and the resistance of the structural materials.

It is estimated that half of the existing building stock in Lisbon is composed by old masonry buildings (Ravara *et al*., 2001). The survey 'Censos 2001' promoted by the 'Instituto Nacional de Estatísticas' (INE – National Institute of Statistics, 2002) confirm that approximately 67% of these buildings are in need of structural intervention works and that 10% present a high stage of degradation. The actual degradation of 'Gaioleiro' buildings, coupled with their weak original condition, justifies the assessment of their seismic vulnerability and the study of rehabilitation procedures.

REFERENCES

(AFML) Arquivo Municipal de Lisboa – Núcleo Fotográfico, Rua da Palma, Lisboa, Portugal.

(Andrade, 2011) Andrade, H. – *Characterization of Old Buildings. 'Gaioleiro' Buildings* (Original Title: *Caracterização de Edifícios Antigos. Edifícios "Gaioleiros"*). M.Sc. Thesys in Civil Engineering, Faculdade de Ciência e Tecnologia da Universidade Nova de Lisboa, March 2011, Monte da Caparica, Portugal (in Portuguese).

(Appleton, 2008) Appleton, J. – *Rehabilitation Design of 'Pombalino' Buildings* (Original Title: *Projecto de Reabilitação de Edifícios Pombalinos*) – *Class paper support*. Appleton Square, March 2008, Lisbon, Portugal (in Portuguese).

(Appleton, 2005) Appleton, J. G. – *Rehabilitation of 'Gaioleiro' Buildings* (Original Title: *Reabilitação de Edifícios "Gaioleiros"*). Orion Edition, 1st Edition, May 2005, Amadora, Portugal (in Portuguese).

(Appleton, 2003) Appleton, J. – *Ancient Buildings Rehabilitation. Pathologies and Intervention Techniques* (Original Title: *Reabilitação de Edifícios Antigos. Patologias e Técnicas de Intervenção*). Orion Edition, 1st Edition, September 2003, Amadora, Portugal (in Portuguese).

(Appleton, 2001) Appleton, J. G. – *Rehabilitation of 'Gaioleiro' Buildings*. *Study of a Quarter on 'Avenidas Novas'* (Original Title: *Reabilitação de Edifícios Gaioleiros. Estudo de Um Quarteirão* *nas Avenidas Novas*). M.Sc. Thesys in Construction, Instituto Superior Técnico, Universidade Técnica de Lisboa, January 2001, Lisbon, Portugal (in Portuguese).

(Branco, 2007) Branco, M – *Seismic Strengthening of Masonry Buildings. Application to 'Gaioleiros' buildings* (Original Title: *Reforço Sísmico de Edifícios de Alvenaria. Aplicação a edifícios "Gaioleiros"*). M.Sc. Thesys in Civil Engineering, Instituto Superior Técnico, Universidade Técnica de Lisboa, October 2007, Lisbon, Portugal (in Portuguese).

(Branco and Correia, 2003) Branco, F.; Correia, J. – *Compression Tests of Masonry Walls from Campo Pequeno Bullring* (Original Title: *Ensaios à Compressão de Elementos de Parede de Alvenaria da Praça de Touros do Campo Pequeno*). Study for SRUCP, ICIST EP Report N.º 82/03, Instituto Superior Técnico, Universidade Técnica de Lisboa, December 2003, Lisbon, Portugal (in Portuguese).

(Candeias, 2008) Candeias, P. – *Assessment of the Seismic Vulnerability of Masonry Buildings* (Original Title: *Avaliação da Vulnerabilidade Sísmica de Edifícios de Alvenaria*). PhD Thesys in Structural Engineering, Universidade do Minho, July 2008, Guimarães, Portugal (in Portuguese).

(Cardoso *et al*., 2005.I) Cardoso, R.; Lopes, M.; Bento, R. – *Seismic evaluation of old masonry buildings. Part I: Method description and application to a case-study*. Engineering Structures, Volume 27, Issue , pp. 2024-2035, September 2005. Available at http://www.sciencedirect.com.

(Cardoso *et al*., 2005.II) Cardoso, R.; Lopes, M.; Bento, R. – *Seismic evaluation of old masonry buildings. Part II: Analysis of strengthening solutions for a case study*. Engineering Structures, Volume 27, Issue, pp. 2014-2023, August 2005. Available at http://www.sciencedirect.com.

(Carvalho and Oliveira, 1997) Carvalho, E. C.; Oliveira, C. S. – *Anti-Seismic Construction – Small buildings* (Original Title: *Construção Anti-Sísmica – Edifícios de Pequeno Porte*). ICT, Informação Técnica de Estruturas, Laboratório Nacional de Engenharia Civil (LNEC), DIT 12, 1997, Lisbon, Portugal (in Portuguese).

(Costa and Oliveira, 1989) Costa, M. G.; Oliveira, C. S. – *Seismic Behaviour of Old Buildings Implanted in Block* (Original Title: *Comportamento Sísmico de Edifícios Antigos Implantados em Quarteirão*). Proceedings of the 1st Seismology and Seismic Engineering Meeting, Laboratório Nacional de Engenharia Civil (LNEC), November 6-7, 1989, Lisbon, Portugal (in Portuguese).

(DIANA®) DIANA® - *DIsplacement method ANAlyser*. Release 9.1, Netherland.

(INE, 2002) Instituto Nacional de Estatísticas (INE) – *Census 2001. Final Results – Lisbon* (Original Title: *Censos 2001. Resultados Definitivos – Lisboa*). Instituto Nacional de Estatísticas (INE), 2002, Lisbon, Portugal (in Portuguese).

(Gomes, 2011) Gomes, R. – *Structural System of Lisbon Ancient Buildings – The 'Pombalino' Buildings and the 'Gaioleiro' Buildings* (Original Title: *Sistema Estrutural de Edifícios Antigos de*

Lisboa – Os Edifícios "Pombalinos" e os Edifícios "Gaioleiros"). M.Sc. Thesys in Civil Engineering, Instituto Superior Técnico, Universidade Técnica de Lisboa, September 2011, Lisbon, Portugal (in Portuguese).

(Jesus, 2007) Jesus, C. – *Seismic Vulnerability of a 'Gaioleiro' Building. Strengthening Solutions* (Original Title: *Vulnerabilidade Sísmica de um Edifício "Gaioleiro". Propostas de Reforço*). M.Sc. Thesys in Civil Engineering, Instituto Superior Técnico, Universidade Técnica de Lisboa, September 2007, Lisbon, Portugal (in Portuguese).

(Lopes *et. al*., 2008) Lopes, M.; Raimundo, M.; Fonseca, J.; Oluveira, C. S.; Azevedo, J.; Bento, R.; Proença, J.; Guerreiro, L.; Appleton, J.; Oliveira, M.; Costa, A.; Carvalho, E.; Leite, A.; Fragoso, M.; Miranda, M.; Casanova, A. – *Earthquakes and Buildings* (Original Title: *Sismos e Edifícios*). Orion Edition, 1st Edition, July 2008, Amadora, Portugal (in Portuguese).

(Lopes and Azevedo, 1997) Lopes, M.; Azevedo, J. – *Assessment of the seismic behaviour of a Lisbon masonry building* (Original Title: *Avaliação do Comportamento Sísmico de um edifício de alvenaria de Lisboa*). Proceedings of the 3rd Seismology and Seismic Engineering Meeting, Instituto Superior Técnico, Universidade Técnica de Lisboa, 1997, Lisbon, Portugal (in Portuguese).

(Mendes and Lourenço, 2009) Mendes, N.; Lourenço, P. – *Seismic Assessment of Masonry "Gaioleiro" Buildings in Lisbon, Portugal*. Journal of Earthquake Engineering, Volume 14, Issue 1, pp. 80-101. Available at http://dx.doi.org/10.1080/13632460902977474.

(Milošević *et al*., 2012) Milošević, J., Gago, A., Bento, R., Lopes, M. – *Experimental Evaluation of the Shear Strength of Masonry Walls*. Proceedings of the 15th International Conference on Experimental Mechanics, Paper N.º 3023, Faculdade de Engenharia da Universidade do Porto, July 2012, Porto, Portugal.

(Pena, 2008) Pena, F. – *Assessment of the Seismic Behaviour of a 'Pombalino' Building* (Original Title: *Avaliação do Comportamento Sísmico de um Edifício Pombalino*). M.Sc. Thesys in Structural Engineering, Instituto Superior Técnico, Universidade Técnica de Lisboa, October 2008, Lisbon, Portugal (in Portuguese).

(Ravara *et al*., 2001) Ravara, A.; Oliveira, C. S.; Carvalho, E.; Lopes, M.; Costa, P.; Delgado, R.; Bairrão, R.; Silva, V. C. – *Reducing the Seismic Vulnerability of the Building Stock*. Ordem dos Engenheiros, Sociedade Portuguesa de Engenharia Sísmica (SPES) and Grémio das Empresas de Conservação e Restauro do Património Arquitectónico (GECoRPA), April 2001, Lisbon, Portugal.

(RSA, 1983) – Safety Regulations and Actions for Buildings and Bridges Structures (Original Title: *Regulamento de Segurança e Acções em Estruturas de Edifícios e Pontes (RSA)*). Decreto-Lei N.º 235/83 de 31 de Maio, Imprensa Nacional Casa da Moeda (INCM), 1983, Lisbon, Portugal (in Portuguese).

(Salvado, 2009) Salvado, A. – *Seismic Assessment of an Old Stone Masonry Building* (Original Title: *Análise Sísmica de um Edifício Antigo em Alvenaria de Pedra*). M.Sc. Thesys in Civil Engineering, Instituto Superior Técnico, Universidade Técnica de Lisboa, February 2009, Lisbon, Portugal (in Portuguese).

(SAP2000®) SAP2000® – *Three Dimensional Static and Dynamic Finite Element Analysis and Design of Structures*. Computers & Structures, Inc. (CSI), Structural and Earthquake Engineering Software, Berkeley, Califórnia, USA..

(SEVERES Project, 2011) SEREVES Project – *Experimental Tests*. PTDC/ECM/100872/2008 - Seismic Vulnerability of Old Masonry Buildings.

(Silva, 2007) Silva, V. C. – *Structural Rehabilitation of Old Buildings. Masonry and Wood. Less Intrusive Techniques* (Original Title: *Reabilitação Estrutural de Edifícios Antigos. Alvenaria e Madeira. Técnicas Pouco Intrusivas*). Argumentum, Grémio das Empresas de Conservação e Restauro do Património Arquitectónico (GECoRPA), 2nd Edition, May 2007, Lisbon, Portugal (in Portuguese).

(Silva and Soares, 1997) Silva, V. C.; Soares, I. – *Seismic Vulnerability of Lisbon 'Gaioleiro' buildings and retrofitting measures* (Original Title: *Vulnerabilidade sísmica dos edifícios "Gaioleiros" de Lisboa e medidas possíveis para a reduzir*). 3rd Seismology and Seismic Engineering Meeting, Laboratório Nacional de Engenharia Civil (LNEC), 1997, Lisbon, Portugal (in Portuguese).

(Technique Tables, 2003) J. S. Farinha B; M. Farinha B; J. P. Farinha B; A. Correia Dos Reis – Technique Tables (Original Title: Tabelas Técnicas). Edições Técnicas E. T. L," LDA, 2003 (in Portuguese).

ANNEX A – 'GAIOLEIRO' BUILDINGS

Table 10 and Table 11 present a summary of the main features of the 'Gaioleiro' buildings.

Table 10 – General data on 'Gaioleiro' buildings.

Date	End of XIX century and beginning of XX century
Location	Liberdade Avenue, Almirante Reis Avenue and 'Avenidas Novas' adjacent to Fontes Pereira de Melo Avenue and República Avenue 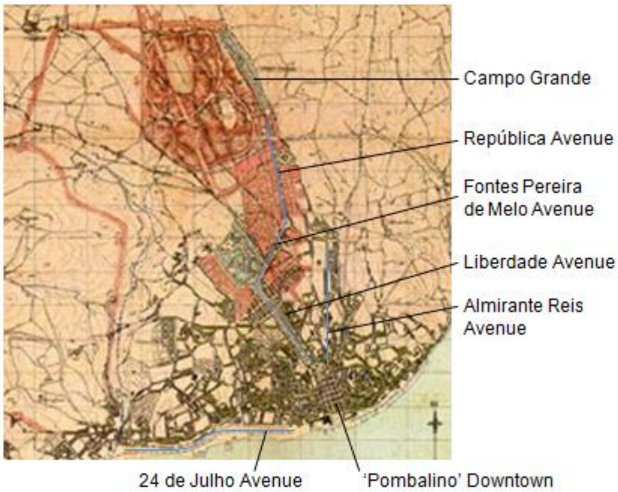
Plan Design	 Rectangular Plan 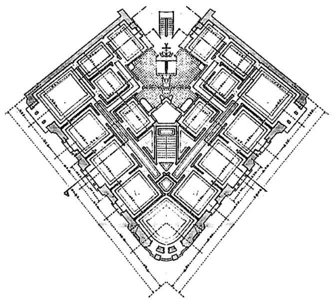 Trapezoidal Plan
Elevation Design	 Front Façade Wall  Back Wall
Number of Floors	5-8

Table 11 - ‘Gaioleiro’ building’s structure.

Foundation	Rubble stone masonry and air lime mortar walls. Thickness reference dimensions: (i) below façade walls: 1.10 to 1.50 m; (ii) below side and light-shaft walls: 0.60 m to 0.70 m.	
Exterior Walls	Rubble stone masonry and air lime mortar walls with decreasing thickness. Reference dimensions on the bottom of the wall: (i) front walls: 0.60 to 0.80 m; (ii) back wall: 0.50 to 0.60 m; (ii) side and light-shaft walls: 0.40 to 0.50 m.	
	Façade walls in rubble stone masonry and side and light-shaft walls in brick masonry with constant thickness between 0.30 to 0.15 m.	
Interior Walls	Brick masonry walls (solid or hollow) with decreasing thickness along the height of the building by changing the position of the bricks.	
	‘Tabique’ walls, originally used as partition walls, have a structural role on the superior floors.	
Floors	Flexible wooden floor diaphragms. Main beams with 0.07 to 0.08 m width and 0.16 to 0.22 m height disposed 0.35 to 0.40 m apart.	
Back Balconies	Iron beams in shape of I or T profile (around 0.20 m height) and brick masonry disposed in vaults.	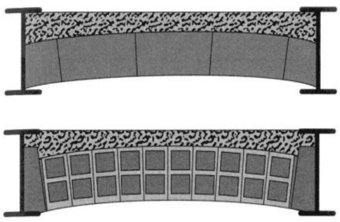

Study: Branco (2007) – *Seismic Strengthening of Masonry Buildings. Application to 'Gaioleiro' buildings*.

Description: The study considered a three dimensional numerical model representative of an existing 'Gaioleiro' building (Figure 37) based on Finite Elements Method, making use of the software SAP2000® (Figure 38). The model was tested and calibrated based on in-situ dynamic characterization tests. Table 12 resumes the main mechanical and geometrical properties of the structural materials and elements of the building and Table 13 the finite elements used on the numerical model of the building.

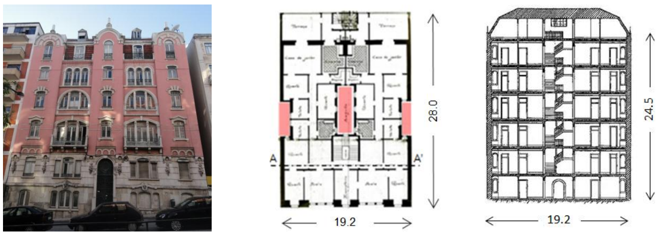

a) b) c)

Figure 37 – 'Gaioleiro' building located on Duque de Loulé Avenue (Branco, 2007): a) Façade wall; b) Plan of a current floor; c) Cross section A-A'.

Table 12 – Mechanical and Geometrical properties of the building.

Structural Material	Mechanical Properties	Structural Element	Dimension
Rubble Stone Masonry	γ = 22.4 kN/m^3 E ([5]) = 1000 MPa ν = 0.2 ξ = 5%	Front Façade Wall	0.90 m (<4th floor) 0.80 m (> 4th floor)
		Back Façade Wall Side Walls	0.60 m (<4th floor) 0.50 m (>4th floor)
	f_c = 4.00 MPa ([6]) f_t = - 0.40 MPa ([6]) τ = 0.14 MPa ([6])	Central Light-Shaft Walls	0.40 m
		Lateral Light-Shaft Walls	0.50 m
Hollow Brick Masonry([7])	γ = 14.9 kN/m^3 E ([5]) = 500 MPa ν = 0.2 ξ = 5%	Staircase Walls (Back Façade Wall)	0.30 m
		Interior Walls (Basement)	
'Tabique' Wall	Square strips nailed to vertical 0.15 m stripes filled on the breaks by rubble masonry	Interior Walls	0.10 m
Pine Wood	γ = 6 kN/m^3 E = 6000 MPa ν = 0.2	Main Beams	0.18 x 0.08 m^2 0.40 m apart
		Secondary Beams	0.08 x 0.08 m^2

[5] The Young's Modulus (E) was determined by calibration of the numerical model with the results of the in-situ dynamic characterization tests.
[6] Results from Costa and Oliveira (1989).
[7] The available results are referred to solid brick masonry (Branco and Correia, 2003).

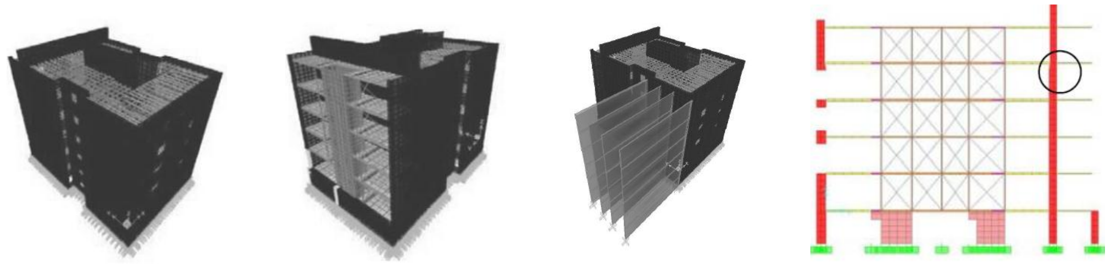

a) b) c) d)

Figure 38 - Numerical Model (Branco, 2007): a) Global model of the building; b) Back façade wall with the ceramic brick balconies; c) Final model taking into account the adjacent reinforced concrete building; d) Cross section of the building with the reduction of the masonry wall thickness between the 4th and the 5th floor.

Table 13 – Finite Elements used on the numerical model.

Finite Element	Modelling	Observations
Volume (8 joints)	Exterior Masonry Walls (Rubble Stone Masonry)	– The distortion deformation of the volume elements is closer to the behaviour of masonry walls; – Visualization of the stress distribution on the wall and along the thickness of the wall; – The weight was defined on the materials properties.
Shell (4 joints) Membrane and plate behaviour	Basement Interior Walls Back Staircase Walls (Brick Masonry Walls)	– The weight was defined on the materials properties.
	Back Balconies Floor (Iron beams and brick masonry)	– Behaviour close to a reinforced concrete slab; – The weight was defined uniform distributed on the floor level.
Frame (2 joints) Beam-Colum behaviour	'Tabique' Walls	– The room division walls were modelled to ensure the support of the floors and to create some lateral locking to the exterior masonry walls; – Frame structure braced by two diagonal joists; – The frame section was based on the results from the shear failure tests performed on 'tabique' walls (Lopes and Azevedo 1997); – The weight was uniform distributed on the floors in order to minimize local vibration modes on the vertical non-resistant elements.
	Timber Floor	– Grid of frame elements taking into account the spacing between the structural elements on numerical model and their actual distribution; – The weight also took into account an equivalent density for each set of spacing and was defined uniform distributed on the floor level.

Study: Jesus (2007) – *Seismic Vulnerability of a 'Gaioleiro' Building. Strengthening Solutions.*

Description: The study considered a three dimensional numerical model representative of an existing 'Gaioleiro' building (Figure 39) based on Finite Elements Method, making use of the software SAP2000® (Figure 40 and Figure 41). The model was tested and calibrated based on in-situ dynamic characterization tests. Table 14 resumes the main mechanical and geometrical properties of the structural materials and elements of the building and Table 15 the finite elements used on the numerical model of the building.

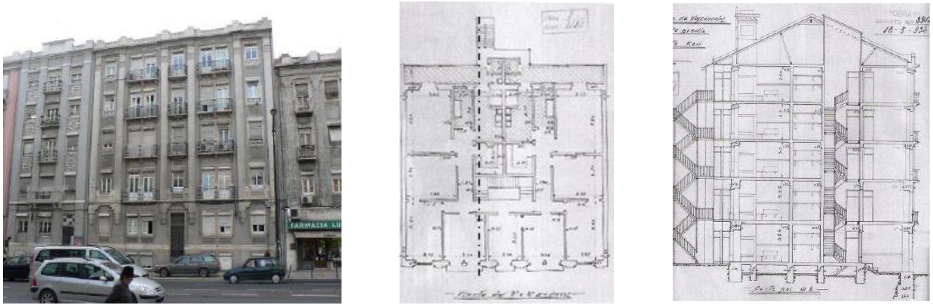

a) b) c)

Figure 39 – ‘Gaioleiro’ building located at Almirante Reis Avenue (Jesus, 2007): a) Front façade wall; b) Plan of a current floor; c) Longitudinal cross section.

Table 14 - Mechanical and Geometrical Properties of the building.

<table>
<tr><th>Structural Material</th><th colspan="2">Mechanical Properties</th><th>Structural Element</th><th colspan="2">Dimension</th></tr>
<tr><td rowspan="7">Rubble Stone Masonry</td><td rowspan="5">Good Quality Masonry Wall</td><td rowspan="3">γ = 22.0 kN/m^3
E ([8]) = 4000 MPa
ν = 0.2</td><td rowspan="5">Façade Wall</td><td>Ground Floor</td><td>0.80 m</td></tr>
<tr><td>1st Storey</td><td>0.70 m</td></tr>
<tr><td>2nd Storey</td><td>0.60 m</td></tr>
<tr><td rowspan="2">f_c = 8.0 MPa
f_t = - 0.20 MPa
τ = 0.40 MPa</td><td>3rd Storey</td><td>0.50 m</td></tr>
<tr><td>4th Storey</td><td>0.50 m</td></tr>
<tr><td rowspan="2">Medium Quality Masonry Wall</td><td>γ = 22.0 kN/m^3
E = 600 MPa
ν = 0.2</td><td rowspan="2">Side Walls</td><td>Ground Floor – 1st Storey</td><td>0.45 m</td></tr>
<tr><td>f_c = 0.90 MPa
f_t = - 0.10 MPa
τ = 0.10 MPa</td><td>2nd Storey – 4th Storey</td><td>0.40 m</td></tr>
<tr><td rowspan="5">Solid Brick Masonry</td><td rowspan="3">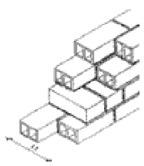</td><td>γ = 3.75 kN/m^3
E ([8]) = 3200 MPa
ν = 0.2</td><td>Interior Walls from the ground floor</td><td colspan="2" rowspan="3">0.25 m</td></tr>
<tr><td rowspan="2">f_c = 5.00 MPa
f_t = - 0.10 MPa
τ = 0.20 MPa</td><td>1st and 2nd storey walls parallel to the façade walls</td></tr>
<tr><td>Staircase Walls</td></tr>
<tr><td rowspan="2">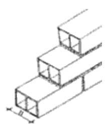</td><td>γ = 2.10 kN/m^3
E ([8]) = 3200 MPa
ν = 0.2</td><td>1st and 2nd storey walls perpendicular to the façade walls</td><td colspan="2" rowspan="2">0.15 m</td></tr>
<tr><td>f_c = 5.00 MPa
f_t = - 0.10 MPa
τ = 0.20 MPa</td><td>3rd and 4th storey walls</td></tr>
<tr><td rowspan="2">Pine Wood</td><td colspan="2" rowspan="2">E = 8000 MPa
ν = 0.2</td><td>Main Beams</td><td colspan="2">0.18 x 0.08 m^2
0.40 m apart</td></tr>
<tr><td>Secondary Beams</td><td colspan="2">0.18 x 0.08 m^2</td></tr>
</table>

[8] The Young’s Modulus (E) was determined by calibration of the numerical model with the results of the in-situ dynamic characterization tests.

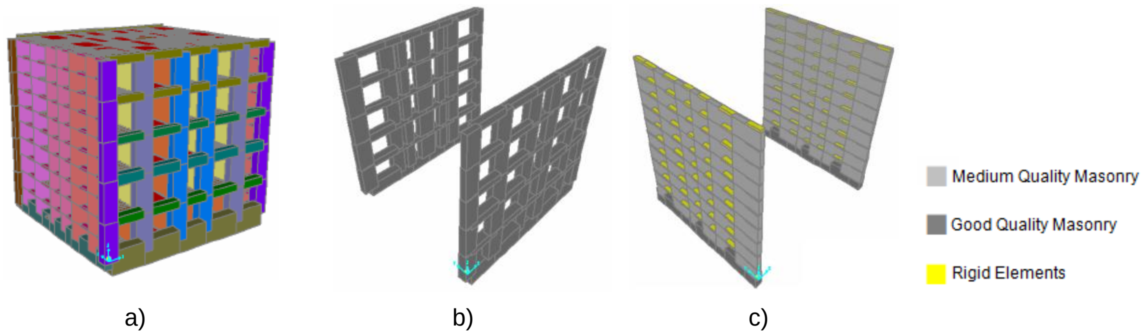

Figure 40 - Numerical Model (Jesus, 2007): a) Global model of the building; b) Model of the façade walls; c) Model of the gable walls (rigid elements).

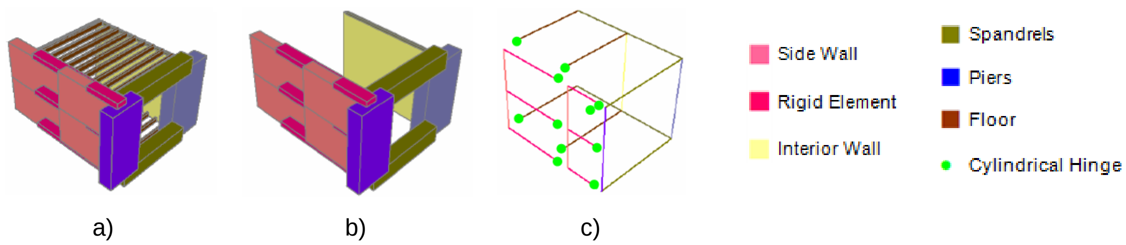

Figure 41 – Numerical Model (Jesus, 2007): a) Floor beams; b) Interior Wall; c) Frame Elements.

Table 15 – Finite Elements used on the numerical model.

<table>
<tr><th>Finite Element</th><th>Modelling</th><th>Observations</th></tr>
<tr><td rowspan="4">Frame
(2 joints)
Beam-Column behaviour</td><td>Façade Masonry Walls</td><td>– Vertical frame elements modelling the piers;
– Horizontal frame elements modelling the spandrels;
– The weight was defined on the materials properties.</td></tr>
<tr><td>Side Masonry Walls</td><td>– Several vertical frame elements connected by horizontal rigid elements at the floor level to guarantee the compatibility between the vertical frame elements;
– The weight was defined on the materials properties.</td></tr>
<tr><td>Interior Brick Masonry Walls</td><td>– The weight was defined on the materials properties.</td></tr>
<tr><td>Timber Floor and Stairs</td><td>– The beams were modelled through a grid o bi-articulated frames;
– The weight was defined distributed at the floor level.</td></tr>
</table>

Study: Candeias (2008) – *Assessment of the Seismic Vulnerability of Masonry Buildings.*

Description: The study considered an experimental campaign developed on 'Laboratório Nacional de Engenharia Civil' (LNEC – National Laboratory of Civil Engineering in Lisbon) considering the seismic vulnerability of 'Gaioleiro' typology of buildings. Five prototypes were built in a reduced scale (1:3) and tested on the LNEC tri-axial shaking table to assess the seismic behaviour of the masonry buildings (Figure 42) and trial the effect of three different reinforcement solutions, represented in Figure 43. Table 16 resumes the main mechanical and geometrical properties of the structural materials and elements of the building.

Figure 42 – Overview of the building prototype before test and test setup (Candeias, 2008).

Model 1 **Model 2** **Model 3**

Figure 43 - Description of the reinforcement solutions (Candeias, 2008): Model 1 - Introduction of metallic connections between masonry walls and floors and fibreglass strips linked with epoxy resins on the front and back façade walls of the 3rd and 4th storey; Model 2 - Connection of opposite masonry walls by tie rods at the floor level; Model 3 - Introduction of fibreglass strips linked with epoxy resins on the front and back façade wall.

The unreinforced prototypes aim to simulate the floors flexibility, the behaviour of the connections between walls and floors and the consequences of the façade openings to the seismic behaviour of these buildings (Model 0). The first reinforced prototype was intended to avoid the collapse of façade walls due to out-of-plane displacements (Model 1 - Figure 43 a). The second reinforced prototype aimed to improve the wall behaviour in its plan through the connection of opposite walls by metallic rods at the floor level (Model 2 - Figure 43 b). The third solution aimed to control generalized cracking on the façade walls related to the low tensile strength of the masonry (Model 3 - Figure 43 c).

Table 16 - Mechanical and Geometrical Properties of the building.

Structural Material	**Mechanical Properties**	**Structural Element**	**Dimension (reduced scale 1:3)**
Self-compacting bentonite-lime concrete	γ = 19.10 kN/m^3 E = 750 MPa υ = 0.20	Façade and Side Walls	0.15 m
	f_c = 0.70 MPa		
Pine Wood	γ = 5.80 kN/m^3 E = 12000 MPa	Main Beams	0.10 x 0.075 m^2 0.25 m apart
		Ring Beams	0.30 x 0.075 m^2
MDF Panels	γ = 7.60 kN/m^3 E = 120 MPa	Floor Boards	0.57 x 1.05 x 0.012 m^3

The dynamic tests were performed on the LNEC shaking table by imposing time series of artificial accelerograms compatible with the design response spectrum defined by the Portuguese Code RSA (1983). The time series were imposed with increasing amplitude (PGA) and in two uncorrelated orthogonal directions (Figure 42 – Test Setup). Before the beginning of the tests and after each time series, the dynamic properties and the damage pattern of the models were characterized.

Study: Salvado (2009) – *Seismic Assessment of an Old Stone Masonry Building.*

Description: The study considered two different numerical models based on the damage distribution of the unreinforced prototype (Model 0 – Candeias, 2008). Firstly, five three dimensional numerical model were developed based on Finite Elements Method, making use of the software SAP2000® (Figure 44 a) to simulate the consecutive experiments performed with the prototype (Candeias, 2008).

The above Table 16 summarizes the main mechanical and geometrical properties of the structural materials and elements of the building, expectation made to the self-compacting bentonite-lime concrete (exterior walls) modulus of elasticity calibrated with the analysis. Table 17 summarizes the finite elements used on the global numerical model of the building.

Table 17 – Finite Elements used on the global numerical model.

Finite Element	Modelling	Observations
Shell (4 joints) Membrane and plate behaviour	Façade and Side Walls	– The weight was defined on the materials properties.
	Floor Boards	– Grid of shell elements with an average area of 0.15 x 0.15 m^2 per element; – The shell elements are simply supported on the floor beams accounting the restrain of the three translation degrees of freedom (xx, yy, zz) and the release of the three rotations degrees of freedom (xx, yy, zz); – The weight was defined distributed at the floor level.
Frame (2 joints) Beam-Column behaviour	Floor Beams	– The end of the beams are supported on the ring beams and accounts the release of two rotations degrees of freedom (xx and yy); – The weight was defined distributed at the floor level.
	Ring Beams	– The ring beams are built-in support the masonry walls; – The connection between perpendicular ring beams accounts the release of two rotations degrees of freedom (xx and yy); – The weight was defined distributed at the floor level.

The building façade wall was then represented by a simplified numerical model based on the equivalent frame method (macro-elements), making use of the software SAP2000® (Figure 44 b). This new model was used to perform a nonlinear static analysis to estimate the capacity curve (pushover curve) of the façade wall in its plane. Table 18 summarizes the main mechanical and geometrical properties of the masonry used on the simplified model and Table

19 summarizes the modelling hypothesis to take into account the nonlinear behaviour of the masonry.

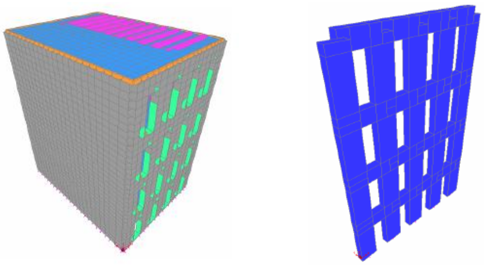

a) b)

Figure 44 - Numerical Model (Salvado, 2009): a) Three dimensional finite model of the building; b) Simplified macro-element model of the façade wall.

Table 18 - Mechanical properties of the rubble masonry used on the simplified model.

Structural Material	Mechanical Properties		Dimension (reduced scale 1:3)
Self-compacting bentonite-lime concrete	γ = 19.1 kN/m^3 E = 750 MPa G = 250 MPa	f_c = 1.00 MPa τ = 0.125 MPa	0.15 m

Table 19 – Macro-Elements used on the simplified numerical model.

Macro-Element	Modelling	Observations	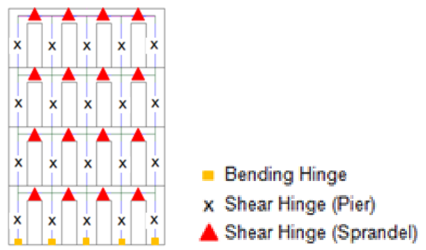
Plastic Hinges	Piers	– One bending hinge at the end of the ground piers (to simulate the connection to the ground foundation); – One shear hinge at mid height.	
	Spandrels	– One shear hinge at mid height.	

Study: Mendes and Lourenço (2009) – *Seismic Assessment of Masonry "Gaioleiro" Buildings in Lisbon, Portugal*.

Description: The study considered the developed the numerical model of the unreinforced prototype (Model 0 – Candeias, 2007) and of the first strengthening solution (Model 1 – Candeias, 2007) using the Finite Element software DIANA® (Figure 45). The behaviour of the building structure was analysed with the purpose of obtaining a crack pattern similar to the one obtained in the tests. The physical nonlinear behaviour of the masonry walls was simulated using the Total Strain Cracking Model detailed in software DIANA® (Table 20 and Figure 46). Then, a safety analysis was performed making use of a nonlinear time history analysis and nonlinear static analysis. After the calibration of the numerical models, it was concluded that the hypothesis of a full translation wall-floor connection was the most appropriate solution with the observed experimental model results (Mendes and Lourenço, 2009). The modelling hypothesis adopted were similar to the ones considered by Salvado (2009), summarized in Table 17.

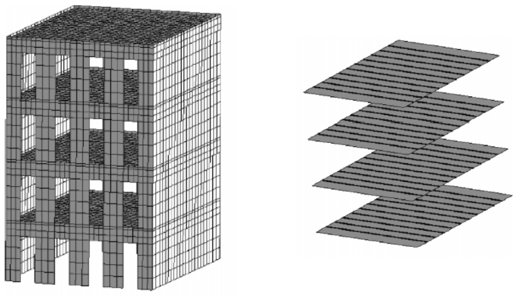

a) b)

Figure 45 – Numerical Model (Mendes and Lourenço, 2009): a) Global view of the building; b) Floor elements.

Table 20 – Nonlinear behaviour of masonry walls.

Structural Material	**Mechanical Properties**		**Modelling Hypothesis**
Self-compacting bentonite-lime concrete	γ = 19.1 kN/m^3 E = 779 MPa υ = 0.2	f_c = 0.80 MPa G'_c = 1.25 N/mm	–Compression behaviour simulated by a parabolic stress-strain relation.
		f_t = 0.125 MPa G'_t = 0.125 N/mm	–Tensile behaviour simulated by an exponential tension-softening relation.
		β = 0.01	–Shear behaviour simulated by a constant retention factor.

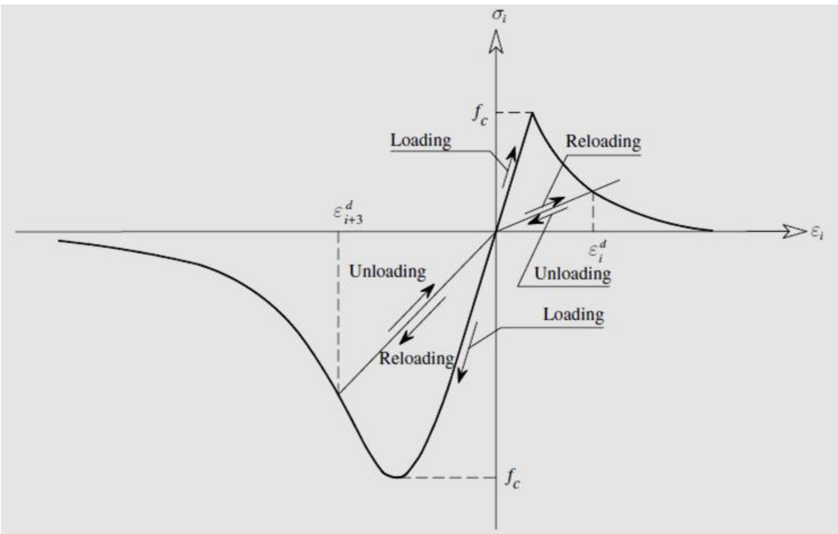

Figure 46 – Adopted hysteretic behaviour of masonry (Mendes and Lourenço, 2009).

Table 21 to Table 24 summarize the main mechanical properties of the structural materials obtained from the case studies referred in section 6 and other bibliographic data related with old masonry buildings.

Table 21 - Rubble Stone Masonry Mechanical Properties.

<table>
<tr><th>Structural Material</th><th colspan="2">Mechanical Properties</th><th colspan="2">Author of the Study</th></tr>
<tr><td rowspan="5">Rubble Stone Masonry</td><td>γ = 24.6 kN/m^3
E = 15000 MPa
ξ = 5%</td><td>f_c = 4.00 MPa
f_t = - 0.40 MPa
τ = 0.14 MPa</td><td colspan="2">Costa and Oliveira (1989)</td></tr>
<tr><td>E = 660 MPa
ξ = 10%</td><td>--</td><td colspan="2">Shear Test
Lopes and Azevedo (1997)</td></tr>
<tr><td>E ϵ [700 - 1000] MPa</td><td>f_c ϵ [0.80 - 1.50] MPa</td><td colspan="2">Bibliographic Data on ‘Gaioleiro’ Buildings
Silva and Soares (1997)</td></tr>
<tr><td>γ = 22.0 kN/m^3
E_i (10) = 3000 MPa
E_f (9) = 1000 MPa
ν = 0.2
ξ = 5%</td><td>f_c = 4.00 MPa (10)
f_t = - 0.40 MPa (11)
τ = 0.14 MPa (11)</td><td colspan="2">Branco (2007)</td></tr>
<tr><td>γ = 22.0 kN/m^3
E = 600 MPa
E (11) = 150 MPa</td><td>f_c = 1.30 MPa
f_t = - 0.10 MPa
τ = 0.10 MPa</td><td colspan="2">‘Pombalino’ Building
Cardoso *et al*. (2005.I)</td></tr>
<tr><td>Good Quality Rubble Stone Masonry</td><td>γ = 22.0 kN/m^3
E_i (10) = 2000 MPa
E_f (10) = 4000 MPa
ν = 0.2</td><td>f_c = 8.00 MPa
f_t = - 0.20 MPa
τ = 0.40 MPa</td><td colspan="2" rowspan="2">Jesus (2007)</td></tr>
<tr><td>Medium Quality Rubble Stone Masonry</td><td>γ = 22.0 kN/m^3
E = 600 MPa
ν = 0.2</td><td>f_c = 0.90 MPa
f_t = - 0.10 MPa
τ = 0.10 MPa</td></tr>
<tr><td rowspan="3">Rubble Stone Masonry with air lime mortar</td><td>E = 563 MPa</td><td>f_c = 7.41 MPa</td><td>Compression Test</td><td rowspan="3">Milošević *et al*., (2012)</td></tr>
<tr><td>G = 57.9 MPa
G = 92.5 MPa</td><td>$\tau_o = f_t$ = 0.024 MPa</td><td>Diagonal Compression Test</td></tr>
<tr><td>--</td><td>τ_o = 0.08 MPa
μ = 0.56</td><td>Triplet Test</td></tr>
</table>

[9] The Young’s Modulus (E) was determined by calibration of the numerical model with the results of the in-situ dynamic characterization tests.
[10] Results from Costa and Oliveira (1989).
[11] Connection between perpendicular masonry walls.

Table 22 - Rubble Stone Masonry Mechanical Properties.

Structural Material	Mechanical Properties		Author of the Study
Self-compacting bentonite-lime concrete	γ = 19.1 kN/m^3 E = 750 MPa υ = 0.20	f_c = 0.70 MPa	Candeias (2008)
	γ = 19.1 kN/m^3 E = 750 MPa G = 250 MPa	f_c = 0.70 MPa τ = 0.125 MPa	Salvado (2008)
	γ = 19.1 kN/m^3 E = 779 MPa υ = 0.2	f_c = 0.80 MPa G'_c = 1.25 N/mm f_t = 0.125 MPa G'_t = 0.125 N/mm β = 0.01	Mendes and Lourenço (2009)

Table 23 - Brick Masonry Mechanical Properties.

Structural Material	Mechanical Properties		Author of the Study
Brick Masonry	γ = 15.68 kN/m^3 E = 5000 MPa	--	Technique Tables (2003)
	γ = 14.60 kN/m^3 E = 5000 MPa	--	Costa and Oliveira (1989)
Campo Pequeno Bull Ring Brick Masonry Walls	E = 330 MPa	--	Compression Test Branco and Correia (2003)
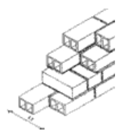	γ = 14.00 kN/m^3 E_i ([12]) = 1000 MPa E_f ([14]) = 500 MPa ν = 0.2 ξ = 5%	--	Branco (2007)
	γ = 3.75 kN/m^3 E_i ([14]) = 1000 MPa E_f ([14]) = 3200 MPa ν = 0.2	f_c = 5.00 MPa f_t = - 0.10 MPa τ = 0.20 MPa	Jesus (2007)
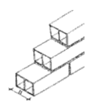	γ = 2.10 kN/m^3 E_i ([14]) = 1000 MPa E_f ([14]) = 3200 MPa ν = 0.2	f_c = 5.00 MPa f_t = - 0.10 MPa τ = 0.20 MPa	Jesus (2007)

In what concerns the data from the case studies listed in section 6, namely Branco (2007) and Jesus (2007), it should be noted that the modulus of elasticity of rubble masonry and brick masonry were adjusted by the calibration of the numerical model developed taking into account the results from the dynamic characterization of the building in analysis, explaining the variability of the values presented.

[12] The Young's Modulus (E) was determined by calibration of the numerical model with the results of the in-situ dynamic characterization tests.

Within the research project SEVERES (www.severes.org) several tests were carried out in the laboratory to assess the mechanical properties of traditional rubble stone masonry (Milošević *et al.*, 2012). Several masonry panels were built with the same materials (limestone and lime mortars) and techniques used in traditional construction and subjected to compression tests, diagonal compression tests and triplet tests.

Nevertheless, the results listed in Table 21 to Table 23 for the masonry (rubble stone and brick) are highly changeable and dispersed, revealing the need of specific and reliable information about the structural materials of 'Gaioleiro' buildings.

Table 24 - Wood Mechanical Properties.

Structural Material	**Mechanical Properties**	**Author of the Study**
Pine Wood	γ = 6 kN/m^3 E = 6000 MPa ν = 0.2	Branco (2007)
	E = 8000 MPa ν = 0.2	Jesus (2007)
	γ = 5.80 kN/m^3 E = 12000 MPa	Candeias (2008)